J Nanopart Res (2012) 14:848
DOI 10.1007/s11051-012-0848-y

RESEARCH PAPER

One-pot fabrication and enhanced thermoelectric properties of poly(3,4-ethylenedioxythiophene)-Bi_2S_3 nanocomposites

Yuan Yuan Wang · Ke Feng Cai · Xi Yao

Received: 10 August 2011 / Accepted: 25 March 2012 / Published online: 8 April 2012

Abstract Bi_2S_3 nanotubes and de-doped poly(3,4-ethylenedioxythiophene) (PEDOT) composite nanopowders were synchronously synthesized by a one-pot self-assembly method. The powders were characterized by X-ray powder diffraction, infrared spectroscopy, and transmission electron microscopy, respectively. Thermoelectric properties of the Bi_2S_3–PEDOT composite nanopowders with different Bi_2S_3 contents after being cold pressed into pellets were measured at room temperature. The sample with 36.1 wt% Bi_2S_3 has a highest power factor of 2.3 $\mu Wm^{-1}K^{-2}$, which is higher than that of both pure PEDOT (0.445 $\mu Wm^{-1}K^{-2}$) and Bi_2S_3 (1.94 $\mu Wm^{-1}K^{-2}$).

Keywords Poly(3,4-ethylenedioxythiophene) · Bi_2S_3 · Nanotubes · Thermoelectric

Y. Y. Wang · K. F. Cai (✉) · X. Yao
Functional Materials Research Laboratory, Tongji University, 1239 Siping Road, Shanghai 200092, China
e-mail: kfcai@tongji.edu.cn

K. F. Cai
State Key Lab of Silicon Materials, Zhejiang University, Hangzhou 310027, China

Introduction

Thermoelectric (TE) materials have recently attracted much attention for their potential applications in power generation, cooling, and thermal sensing. The performance of a TE material is evaluated by the dimensionless figure of merit ZT ($ZT = \alpha^2\sigma T/\kappa$, where T is the absolute temperature, α the Seebeck coefficient, σ the electrical conductivity and κ the thermal conductivity). Although telluride or selenide materials, such as $(Bi, Sb)_2(Te, Se)_3$ (Datta et al. 2010; Venkatasubramanian et al. 2001; Yan et al. 2010), Pb(Te, Se)-based compounds (Harman et al. 2002; Hsu et al. 2004), have good TE property, it is necessary to explore new TE materials because of the toxicity of tellurium and selenium, and the conflict between their less abundance and large consumption in the field of solar cells.

Bismuth trisulfide (Bi_2S_3) with a band gap of 1.3 eV is a layered semiconductor which crystallizes in the *Pbnm* orthorhombic space group. It has recently attracted increasing attention due to its potential application in TE field (Chen et al. 1997; Liufu et al. 2007). TE nanostructures have theoretically and experimentally been shown with enhanced TE properties because of quantum size effect and enhanced interface scattering of phonons (Boukai et al. 2008; Harman et al. 2002; Hicks and Dresselhaus 1993; Hicks et al. 1996; Hochbaum et al. 2008; Venkatasubramanian et al. 2001). Recently, various techniques have been utilized to prepare Bi_2S_3 nanostructures, such as vapor deposition (Ye et al. 2002; Yu and Cao 2008), hydrothermal/solvothermal

synthesis (Chen et al. 2003; Shi et al. 2006), ultrasonic chemical method (Xing et al. 2003; Zhu et al. 2003), electrochemical method (Huang et al. 2008), microwave-assisted route (He et al. 2003), surfactant-assisted approach (Li et al. 2002), and high temperature (120–180 °C) chemical method in solution of oleic acid and oleylamine (8:3) (Ibáñez et al. 2011). These methods usually require expensive apparatus or relative complicated process. In this study, we developed a facile route to prepare Bi_2S_3 nanotubes in aqueous solution at room temperature and atmosphere pressure.

Besides traditional inorganic TE materials, increasing attention has been paid to organic materials, especially conjugated polymers such as polyaniline, polypyrrole, polythiophene (PTh) and their derivatives (Feng and Ellis 2003; Jiang et al. 2008; Kaiser 2001; Li et al. 2010; Sun et al. 2010; Toshima 2002), as they possess a number of advantageous properties including low density, low thermal conductivity, low cost, and ease of synthesis and processing into versatile forms. One of the PTh derivatives, poly(3,4-ethylenedioxythiophene) (PEDOT) becomes more and more important due to its low redox potential, high electrical conductivity, and good environmental stability. The thermal conductivity of the PEDOT is usually lower than that of inorganic materials, which is good to increase ZT value. Unfortunately, the ZT value of PEDOT is still much lower than that of traditional TE materials (Jiang et al. 2008).

It is reported that introducing a highly electrical conducting secondary phase into a material to increase the electrical conductivity while not negatively affecting the Seebeck effect can improve TE properties (Mori et al. 2007). Fabricating polymer-inorganic TE nanocomposite materials may be a good way to obtain high TE properties, as the composite may inherit the properties of both the polymer and inorganic nanostructures (Yao et al. 2010; Yu et al. 2008). Recently, several contributions have devoted to the PEDOT based hybrid TE materials. For example, Kim et al. reported that enhanced TE property could be obtained by filling carbon nanotubes into PEDOT:PSS [poly(styrenesulfonate)] (Kim et al. 2010). The composite has much higher electrical conductivities than the pure PEDOT:PSS without significantly altering Seebeck coefficient. Zhang et al. incorporated ball milled Bi_2Te_3 powders into commercialized PEDOT:PSS products and the composite material showed outstanding power factor of 70 $\mu Wm^{-1}K^{-2}$ (Zhang et al. 2010). See et al. reported a film consisting of PEDOT:PSS functionalized Te nanorods prepared directly from water, and the ZT value of the hybrid film reaches about 0.1 at room temperature, which is the highest ZT value of aqueous processed materials (See et al. 2010).

In our previous study, we have synthesized PbTe-modified de-doped PEDOT nanotubes by first preparing PbTe nanoparticles and then in situ polymerization at n-hexane/acetonitrile interface (Wang et al. 2011). This work presents a one-pot self-assembly method to prepare Bi_2S_3 nanotubes and PEDOT composite powders. The electrical conductivity and Seebeck coefficient of the composite powders after cold pressing were measured at room temperature.

Experimental

The 3,4-ethylenedioxythiophene (EDOT) monomer was purchased from Suzhou Yield Pharma Co. Ltd., China, and other reagents were purchased from Sinopharm Chemical Reagent Co. Ltd., China. All reagents were analytical grade and directly used without further purification.

Synthesis of PEDOT

In a typical run, 10 mmol $(NH_4)_2S_2O_8$ (APS) was dissolved in 50 mL 2 mol/L nitric acid, and the solution was called solution A. 1 mL ($\approx$ 10 mmol) of EDOT was dissolved in 50 mL isopropanol, and the solution was called solution B. Solution A was dropped into the solution B at one drop every 2 s, followed by stirring for 4 h at room temperature. Then the solution was placed at room temperature without stirring for about 20 h. The product was collected from the polymerization media by centrifugation and rinsed with deionized water and absolute ethanol in sequence for several times, then separated by centrifugation for 5 min at 4,000 rpm and finally dried in vacuum at 70 °C. The product is called sample IA. Some of the sample IA was treated with 0.2 M ammonium hydroxide to become de-doped PEDOT, which is called sample IB.

Synthesis of Bi_2S_3 nanotubes

In a typical run, 2 mmol $Bi(NO_3)_3{\cdot}5H_2O$ and 3 mmol thioacetamide were dissolved in 100 mL 1 mol/L

nitric acid. The solution was called solution C. The solution was placed at room temperature without stirring. About 24 h later, there were black precipitates at the bottom of the beaker. The black precipitates were washed with deionized water and absolute ethanol in sequence for several times, then separated by centrifugation for 5 min at 4,000 rpm and finally dried in vacuum at 70 °C. The yield was ~91 %. The product is called sample II.

One-pot fabrication of PEDOT-Bi_2S_3 composite nanopowders

A typical synthetic process of PEDOT-Bi_2S_3 composite nanopowders was performed as follows: 25 mL solution A, 25 mL solution B, and 20 mL solution C was prepared, respectively. Solution A was dropped into solution B at one drop every 2 s, then solution C was added into the mixture of solutions A and B followed by stirring for 4 h at room temperature. After that the mixed solution was placed at room temperature without stirring for about 20 h. The precipitate obtained at the bottom of the beaker was washed with deionized water, ammonium hydroxide, absolute ethanol in sequence for several times, then separated by centrifugation for 5 min at 4,000 rpm and finally dried in vacuum at 70 °C. The product is called sample III. The Bi_2S_3 content (c) was estimated on the basis of yield of sample II (91 %) and calculated by the equation: $c = (w1 \times 91\ \%)/w \times 100\ \%$, where $w1$ is the theoretical weight of Bi_2S_3 generated in the reaction system and w the weight of the final product. Bi_2S_3 content in the sample III was estimated to be ~17.8 wt%.

This procedure was repeated but adding 30, 40, and 50 mL solution C, respectively. The Bi_2S_3 content in the corresponding composite powder was estimated to be 25.0, 30.2, and 36.1 wt%, respectively.

The synthesis conditions of all samples were briefly listed in Table 1.

Characterization

Samples IB, II and III were examined by X-ray diffraction (XRD) performed on a Bruker D8 Advanced X-ray Diffractometer with Cu K_α radiation ($\lambda = 1.5406$ Å). FTIR spectroscopy was used to characterize the molecular structure of samples IA, IB, and III. The morphology of samples II and III was observed with transmission electron microscopy (TEM, Hitachi H-800). The powder samples were cold pressed into pellets (10 mm in diameter and about 1 mm in thickness) at ~10 MPa for electrical conductivity and Seebeck coefficient measurement. The bulk electrical conductivity of each pellet was measured by a two-probe method: the pellet was sandwiched with two round-disk copper electrodes. The Seebeck coefficient was determined by the slope of the linear relationship between the thermal electromotive force and temperature difference (~10–15 K) between the two sides of each pellet. The error of the measured Seebeck coefficient values is <10 %.

Results and discussion

Figures 1a, b and c show XRD patterns of samples IB, II and III, respectively. The pattern of sample IB (Fig. 1a) is a typical amorphous pattern with a low and broad peak at about 23°, due to its poor crystallinity. All the diffraction peaks for sample II can be indexed to the reported Bi_2S_3 (JCPDS card file, No. 89-8964) with the *Pbnm* space group. The XRD pattern of sample III is quite similar to that of sample II. A weak peak at about 23° (marked by a star) can also be found in the XRD pattern of sample III. Therefore, the composite mainly consists of two phases: Bi_2S_3 and PEDOT.

Figure 2a shows the infrared spectrum of sample IA, which corresponds to that for PEDOT. The peaks at 688, 835, and 979 cm^{-1} are assigned to C–S bond

Table 1 The synthesis condition for each sample

Samples	Composition	Synthesis media	Doped/dedoped
Sample IA	PEDOT	Mixture of isopropanol and H_2O	HNO_3-doped
Sample IB	PEDOT	Mixture of isopropanol and H_2O	Dedoped
Sample II	Bi_2S_3	H_2O	–
Sample III	PEDOT-Bi_2S_3	Mixture of isopropanol and H_2O	Dedoped

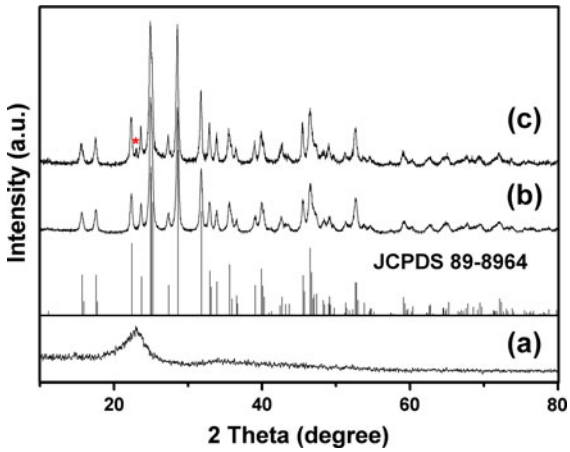

Fig. 1 Typical XRD patterns of the (*a*) sample IB, (*b*) sample II, and (*c*) sample III, the standard XRD data of Bi_2S_3 (JCPDS card file, 89-8964) was also given for comparison

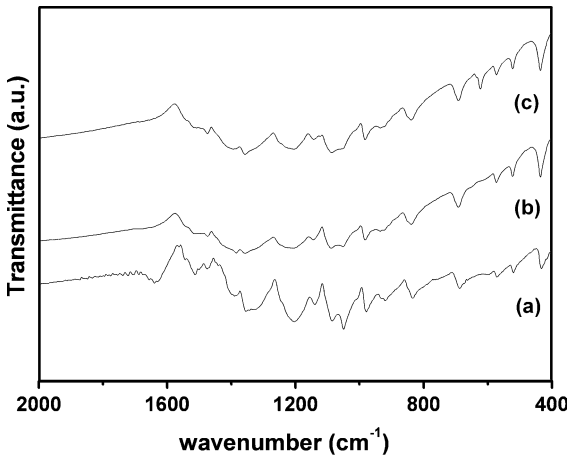

Fig. 2 FT infrared transmission spectra of (*a*) sample IA, (*b*) sample IB, and (*c*) sample III

stretching vibration in thiophene rings, and the absorption peaks at 1,513 and 1,357 cm^{-1} are related to the C–C or C=C stretching of the vibration thiophene rings. The peaks at 1,051, 1,085, and 1,201 cm^{-1} could be attributed to the stretching of –C–O–C– bonds. The absorption peak at 1,641 cm^{-1} indicates that the obtained PEDOT has been doped after polymerizing reaction, which agrees with the result reported in ref. (Groenendaal et al. 2000). There is no adsorption peak at 1,641 cm^{-1} in the spectrum of sample IB (Fig. 2b), indicating a reductive state of the PEDOT. The spectrum for sample III (Fig. 2c) is very similar to that of sample IB. Combining the XRD and FTIR results, it can be deduced that sample III consists of Bi_2S_3 and reductive PEDOT.

Figures 3 a and b show typical TEM images of samples II and III, respectively. It can be seen from Fig. 3 a that sample II mainly consists of one-dimensional (1D) nanostructures. It is seen from the enlarged image (inset in Fig. 3a) of the square zone in Fig. 3a that the nanostructures are in fact nanotubes with diameter of ~80 nm and length of ~500–800 nm. The Bi_2S_3 nanotubes should be longer as they could be broken during the ultrasonic dispersion procedure. The surface of the Bi_2S_3 nanotubes is very smooth and clear. During the reaction procedure,

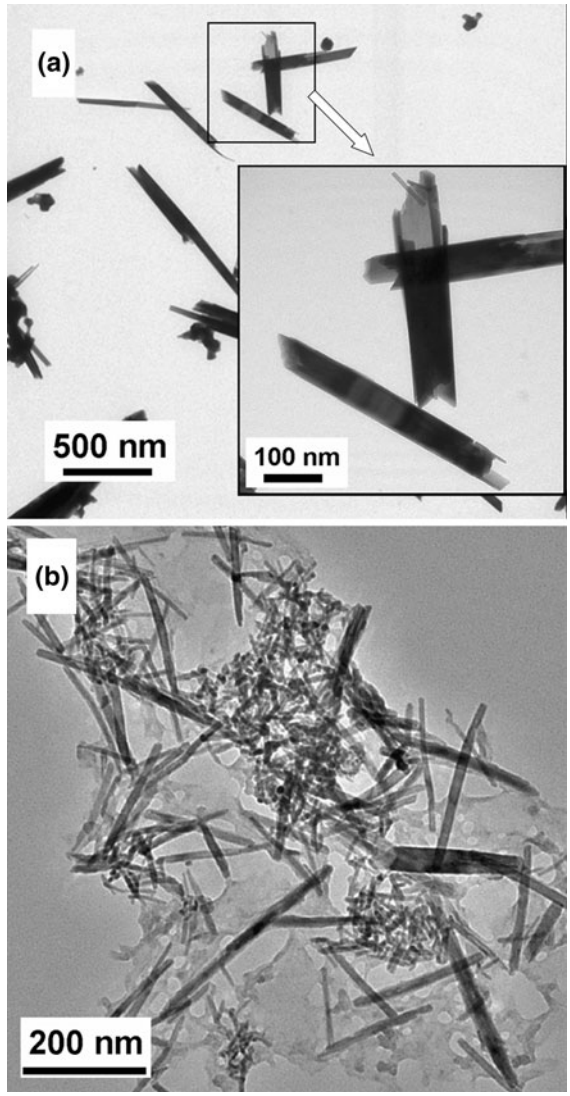

Fig. 3 Typical TEM images of **a** sample II and **b** sample III

the thioacetamide was slowly hydrolyzed in the acidic solution to generate H_2S, and then the H_2S reacted with Bi^{3+} to form Bi_2S_3 nuclei. The nuclei grew up to form Bi_2S_3 nanotubes because of highly anisotropic structure of the orthorhombic Bi_2S_3.

A typical TEM image of the PEDOT–Bi_2S_3 composite nanopowders is shown in Fig. 3b. Bi_2S_3 nanotubes are with dark contrast, while the PEDOT is with lighter contrast. The formation mechanism of the composite nanostructures is suggested as follows: the Bi_2S_3 nanotubes were formed as mentioned above. Meanwhile, EDOT monomer was oxidized by $S_2O_8^{2-}$ and formed PEDOT which coated on the Bi_2S_3 nanotubes. As both the Bi_2S_3 nanotubes and the PEDOT were formed in a homogeneous solution, Bi_2S_3 nanotubes were well dispersed in the PEDOT matrix.

The electrical conductivity, Seebeck coefficient, and power factor of samples IA, IB and II after cold pressing at room temperature are given in Table 2. The electrical conductivity and Seebeck coefficient of sample IA are 348 Sm^{-1} and 16.9 μVK^{-1}, respectively, indicating P-type conduction. The charge carriers of the sample are positive polarons or bipolarons, created upon doping (Furukawa 1996). Compared with sample IA, sample IB has much lower electrical conductivity (0.166 Sm^{-1}) but much larger absolute Seebeck coefficient value (1,637.5 μVK^{-1}). This is because during the dedoping procedure for preparation of sample IB, the counterions (NO_3^-) were removed, which not only leads to a distinctly decrease of carrier concentration, but also changes the type of charge carriers. The calculated power factor of the de-doped PEDOT (0.445 $\mu Wm^{-1}K^{-2}$) is more than four times higher than that of the doped one (0.1 $\mu Wm^{-1}K^{-2}$). The electrical conductivity and Seebeck coefficient of sample II after cold pressing are 37.6 Sm^{-1} and -226.9 μVK^{-1}, respectively, which is lower than that of the bulk Bi_2S_3 reported in ref.(Chen et al. 1997). The low electrical conductivity should be due to large quantity of interfaces which will strongly scatter the transport of carriers.

Table 2 The electrical conductivity, Seebeck coefficient, and power factor ($\alpha^2\sigma$) of samples IA, IB and II at room temperature

Sample	σ (Sm^{-1})	α (μVK^{-1})	$\alpha^2\sigma$ ($\mu Wm^{-1}K^{-2}$)
Sample IA (HNO_3-doped PEDOT)	348	16.94	0.100
Sample IB (de-doped PEDOT)	0.166	−1637.5	0.445
Sample II (Bi_2S_3)	37.6	−226.9	1.94

As the Seebeck coefficient of doped PEDOT is positive while those of de-doped PEDOT as well as Bi_2S_3 are negative, we chose the de-doped PEDOT as the matrix of the composites. All the PEDOT-Bi_2S_3 composite nanopowders are dedoped by ammonium hydroxide. Figure 4 shows the room-temperature electrical conductivity, Seebeck coefficient, and power factor of the composite nanopowders with different amount of Bi_2S_3 after cold pressing. As shown in Fig. 4a, when the Bi_2S_3 content increases from 0 to 36.1 wt%, the electrical conductivity of the samples increases from 0.166 to 1.3 Sm^{-1}, whereas the absolute Seebeck coefficient value first increases from 1,637.5 μVK^{-1} (pure PEDOT) to 1,724 μVK^{-1} (17.8 wt% Bi_2S_3 sample, sample III) and then decreases to 1,318 μVK^{-1} (36.1 wt% Bi_2S_3 sample). The slightly

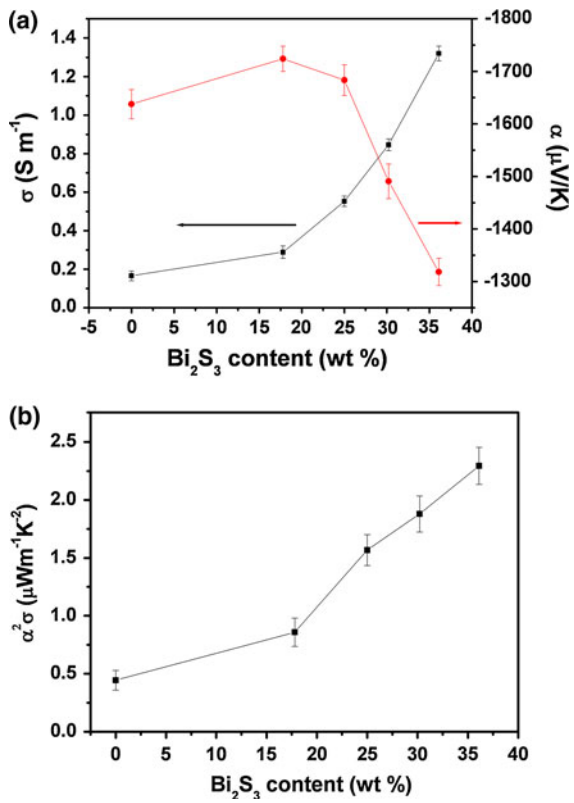

Fig. 4 **a** Electrical conductivities, Seebeck coefficients and **b** power factors ($\alpha^2\sigma$) of the nanocomposites with different Bi_2S_3 content after cold pressing

increase of the Seebeck coefficient at low Bi_2S_3 content is probably due to the special nanostructures and the interface between the PEDOT and Bi_2S_3 nanotubes of the composite powders.

Figure 4b shows that the calculated power factor increases with the Bi_2S_3 content increasing and that the sample with 36.1 wt% Bi_2S_3 has a highest power factor value, 2.3 $\mu Wm^{-1}K^{-2}$, which is higher than that of pure Bi_2S_3 (1.94 $\mu Wm^{-1}K^{-2}$, see Table 2) and five times as large as that of the pure PEDOT (0.445 $\mu Wm^{-1}K^{-2}$), and the power factor still has an increasing trend when the Bi_2S_3 content is about 36.1 wt%. This power factor value is also higher than that of the PbTe nanoparticles modified de-doped PEDOT (1.44 $\mu Wm^{-1}K^{-2}$) reported in ref. (Wang et al. 2011). As inorganic TE component usually has higher TE performance than polymer, the content of inorganic TE nanostructures in the composite should be as high as possible (Du et al. 2012). We believe that further increase the content of Bi_2S_3, the power factor of the composite could be further improved. Compared with state-of-the-art inorganic TE materials, the power factor of the composite is still very low. This is mainly because of the relative low electrical conductivity of Bi_2S_3. Hence, we deduce that a composite consisting of the PEDOT and high electrical conducting 1D nanostructures would have better TE properties.

Conclusions

In summary, a facile one-pot self-assembly route to PEDOT–Bi_2S_3 nanotubes composite powders at room temperature was presented. The pure de-doped PEDOT exhibited large Seebeck coefficient ($-1{,}637.5$ μVK^{-1}), but low electrical conductivity (0.166 Sm^{-1}). As the Bi_2S_3 content increased (up to 36.1 wt%), the electrical conductivity of the composite powder after cold pressing increased, whereas the Seebeck coefficient first increased then decreased, and the power factor monotonically increased. The sample with 36.1 wt% Bi_2S_3 had a highest power factor, 2.3 $\mu Wm^{-1}K^{-2}$, which is about five times as large as that of the pure PEDOT. This work suggests that fabrication of nanocomposites containing de-doped conjugated polymers with large Seebeck coefficient and one-dimensional inorganic TE semiconductors with high electrical conductivity may be an alternative route to TE materials with good properties.

Acknowledgments This work was supported by National Natural Science Foundation of China (50872095), Doctoral Fund of Ministry of Education of China, the foundation of the State Key Lab of Advanced Technology for Materials Synthesis and Processing, Wuhan University of Technology, and Foundation of the State Key Lab of Silicon Materials, Zhejiang University.

References

Boukai AI, Bunimovich Y, Tahir-Kheli J, Yu J-K, GoddardIII WA, Heath JR (2008) Silicon nanowires as efficient thermoelectric materials. Nature 451:168–171

Chen BX, Uher C, Iordanidis L, Kanatzidis MG (1997) Transport properties, of Bi_2S_3 and the ternary bismuth sulfides $KBi_{6.33}S_{10}$ and $K_2Bi_8S_{13}$. Chem Mater 9:1655–1658

Chen Y, Kou HM, Jiang J, Su Y (2003) Morphologies of nanostructured bismuth sulfide prepared by different synthesis routes. Mater Chem Phys 82:1–4

Datta A, Paul J, Kar A, Patra A, Sun ZL, Chen LD, Martin J, Nolas GS (2010) Facile chemical synthesis of nanocrystalline thermoelectric alloys based on Bi–Sb–Te–Se. Cryst Growth Des 10:3983–3989

Du Y, Shen SZ, Cai KF, Casey PS (2012) Research progress on polymer-inorganic thermoelectric nanocomposite materials. Prog Polym Sci. doi:10.1016/j.progpolymsci.2011.11.003

Feng J, Ellis TW (2003) Feasibility study of conjugated polymer nano-composites for thermoelectrics. Synth Met 135: 55–56

Furukawa Y (1996) Electronic absorption and vibrational spectroscopies of conjugated conducting polymers. J Phys Chem 100:15644–15653

Groenendaal BL, Jonas F, Freitag D, Pielartzik H, Reynolds JR (2000) Poly(3,4-ethylenedioxythiophene) and its derivatives: past, present, and future. Adv Mater 12:481–494

Harman TC, Taylor PJ, Walsh MP, LaForge BE (2002) Quantum dot superlattice thermoelectric materials and devices. Science 297:2229–2232

He R, Qian XF, Yin J, Zhu ZK (2003) Preparation of Bi_2S_3 nanowhiskers and their morphologies. J Cryst Growth 252:505–510

Hicks LD, Dresselhaus MS (1993) Effect of quantum-well structures on the thermoelectric figure of merit. Phys Rev B 47:12727–12731

Hicks LD, Harman TC, Sun X, Dresselhaus MS (1996) Experimental study of the effect of quantum-well structures on the thermoelectric figure of merit. Phys Rev B 53: 10493–10496

Hochbaum AI, Chen R, Delgado RD, Liang W, Garnett EC, Najarian M, Majumdar A, Yang P (2008) Enhanced thermoelectric performance of rough silicon nanowires. Nature 451:163–168

Hsu KF, Loo S, Guo F, Chen W, Dyck JS, Uher C, Hogan T, Polychroniadis EK, Kanatzidis MG (2004) Cubic $AgPb_mSbTe_{2+m}$: bulk thermoelectric materials with high figure of merit. Science 303:818–821

Huang XH, Yang YW, Dou XC, Zhu YG, Li GG (2008) In situ synthesis of Bi/Bi_2S_3 heteronanowires with nonlinear electrical transport. J Alloys Compd 461:427–431

Ibáñez M, Guardia P, Shavel A, Cadavid D, Arbiol J, Morante JR, Cabot A (2011) Growth kinetics of asymmetric Bi_2S_3 nanocrystals: size distribution focusing in nanorods. J Phys Chem C 115:7947–7955

Jiang FX, Xu JK, Lu BY, Xie Y, Huang RJ, Li LF (2008) Thermoelectric performance of poly(3,4-ethylenedioxythiophene): poly(styrenesulfonate). Chin Phys Lett 25: 2202–2205

Kaiser AB (2001) Electronic transport properties of conducting polymers and carbon nanotubes. Rep Prog Phys 64:1–49

Kim D, Kim Y, Choi K, Grunlan JC, Yu CH (2010) Improved thermoelectric behavior of nanotube-filled polymer composites with poly(3,4-ethylenedioxythiophene) poly(styrenesulfonate). ACS Nano 4:513–523

Li Q, Shao MW, Wu J, Yu GH, Qian YT (2002) Synthesis of nano-fibrillar bismuth sulfide by a surfactant-assisted approach. Inorg Chem Commun 5:933–936

Li JJ, Tang XF, Li H, Yan YG, Zhang QJ (2010) Synthesis and thermoelectric properties of hydrochloric acid-doped polyaniline. Synth Met 160:1153–1158

Liufu SC, Chen LD, Yao Q, Wang CF (2007) Assembly of one-dimensional nanorods into Bi_2S_3 films with enhanced thermoelectric transport properties. Appl Phys Lett 90:112106

Mori T, Nishimura T, Yamaura K, Takayama-Muromachi E (2007) High temperature thermoelectric properties of a homologous series of n-type boron icosahedra compounds: A possible counterpart to p-type boron carbide. J Appl Phys 101:093714

See KC, Feser JP, Chen CE, Majumdar A, Urban JJ, Segalman RA (2010) Water-processable polymer-nanocrystal hybrids for thermoelectrics. Nano Lett 10:4664–4667

Shi HQ, Zhou XD, Fu X, Wang DB, Hu ZS (2006) Preparation of CdS nanowires and Bi_2S_3 nanorods by extraction-solvothermal method. Mater Lett 60:1793–1795

Sun J, Yeh ML, Jung BJ, Zhang B, Feser J, Majumdar A, Katz HE (2010) Simultaneous increase in seebeck coefficient and conductivity in a doped poly(alkylthiophene) blend with defined density of states. Macromolecules 43: 2897–2903

Toshima N (2002) Conductive polymers as a new type of thermoelectric material. Macromol Symp 186:81–86

Venkatasubramanian R, Siivola E, Colpitts T, O'Quinn B (2001) Thin-film thermoelectric devices with high room-temperature figures of merit. Nature 413:597

Wang YY, Cai KF, Yao X (2011) Facile fabrication and thermoelectric properties of pbTe-modified poly(3,4-ethylenedioxythiophene) nanotubes. ACS Appl Mater Interfaces 3:1163–1166

Xing GJ, Feng ZJ, Chen GH, Yao W, Song XM (2003) Preparation of different morphologies of nanostructured bismuth sulfide with different methods. Mater Lett 57:4555–4559

Yan XA, Poudel B, Ma Y, Liu WS, Joshi G, Wang H, Lan YC, Wang DZ, Chen G, Ren ZF (2010) Experimental studies on anisotropic thermoelectric properties and structures of n-type $Bi_2Te_{2.7}Se_{0.3}$. Nano Lett 10:3373–3378

Yao Q, Chen LD, Zhang WQ, Liufu SC, Chen XH (2010) Enhanced thermoelectric performance of single-walled carbon nanotubes/polyaniline hybrid nanocomposites. ACS Nano 4:2445–2451

Ye CH, Meng GW, Jiang Z, Wang YH, Wang GZ, Zhang LD (2002) Rational growth of Bi_2S_3 nanotubes from quasi-two-dimensional precursors. J Am Chem Soc 124:15180–15181

Yu XL, Cao CB (2008) Photoresponse and field-emission properties of bismuth sulfide nanoflowers. Cryst Growth Des 8:3951–3955

Yu C, Kim YS, Kim D, Grunlan JC (2008) Thermoelectric behavior of segregated-network polymer nanocomposites. Nano Lett 8:4428–4432

Zhang B, Sun J, Katz HE, Fang F, Opila RL (2010) Promising thermoelectric properties of commercial pedot:pss materials and their Bi_2Te_3 powder composites. ACS Appl Mater Interfaces 2:3170–3178

Zhu JM, Yang K, Zhu JJ, Ma GB, Zhu XH, Zhou SH, Liu ZG (2003) The microstructure studies of bismuth sulfide nanorods prepared by sonochemical method. Opt Mater 23:89–92